Review

Andrea Pasquadibisceglie and Fabio Polticelli*

Computational studies of the mitochondrial carrier family SLC25. Present status and future perspectives

https://doi.org/10.1515/bams-2021-0018
Received March 12, 2021; accepted April 7, 2021;
published online April 27, 2021

Abstract: The members of the mitochondrial carrier family, also known as solute carrier family 25 (SLC25), are transmembrane proteins involved in the translocation of a plethora of small molecules between the mitochondrial intermembrane space and the matrix. These transporters are characterized by three homologous domains structure and a transport mechanism that involves the transition between different conformations. Mutations in regions critical for these transporters' function often cause several diseases, given the crucial role of these proteins in the mitochondrial homeostasis. Experimental studies can be problematic in the case of membrane proteins, in particular concerning the characterization of the structure–function relationships. For this reason, computational methods are often applied in order to develop new hypotheses or to support/explain experimental evidence. Here the computational analyses carried out on the SLC25 members are reviewed, describing the main techniques used and the outcome in terms of improved knowledge of the transport mechanism. Potential future applications on this protein family of more recent and advanced *in silico* methods are also suggested.

Keywords: membrane proteins; mitochondrial carrier family; molecular dynamics; protein structure modelling; solute carrier family 25.

***Corresponding author: Fabio Polticelli,** Department of Sciences, Roma Tre University, Viale Guglielmo Marconi 446, 00146 Rome, Italy; and National Institute of Nuclear Physics, Roma Tre Section, Rome, Italy, Phone: +39 06 57336362, Fax: +39 06 57336321, E-mail: fabio.polticelli@uniroma3.it
Andrea Pasquadibisceglie, Department of Sciences, Roma Tre University, Rome, Italy

Introduction

Mitochondria and cytosol are involved in many metabolic processes that require the import/export of fundamental molecules (e.g., adenosine diphosphate (ADP), adenosine triphosphate (ATP), and phosphate for oxidative phosphorylation, substrates for the citric acid cycle, for fatty acid oxidation, for mitochondrial replication, etc.) [1]. Due to the impermeable nature of the inner membrane, only a few neutral molecules (such as O_2 and CO_2) can cross the mitochondrial membranes without protein mediation. The transport of a variety of metabolites, nucleotides, and cofactors through the inner mitochondrial membrane is performed by a family of membrane transporters known as mitochondrial carrier family (MCF) or solute carrier family 25 (SLC25). This family includes solute transporters, such as the mitochondrial tricarboxylate transport protein (SLC25A1) [2], the ADP/ATP translocase (SLC25A4) [3] and the carnitine–acylcarnitine carrier (SLC25A20) [3]. Although big efforts have been made to characterize this protein family (Table 1), a fifth of them still does not have a known function (SLC25A16, SLC25A25, SLC25A34, SLC25A35, SLC25A39, SLC25A40, SLC25A43, SLC25A45, SLC25A46, SLC25A48, SLC25A49, SLC25A50, and SLC25A53).

All MCs have common structural characteristics, different from those of any other SLC family member. The structural feature that makes their identification unequivocal is the presence of three homologous domains repeated in tandem, of about 100 amino acids in length. Each one contains two hydrophobic regions, separated by a large hydrophilic sequence. In detail, the structure is composed of six transmembrane α-helices (H1 to H6), linked by three short α-helices (h12, h34 and h56) on the matrix side, forming a funnel-shaped structure with the cavity open towards the cytosol and closed on the side of the matrix. Proline residues of the conserved Px[DE]xx[RK] signature motifs make contact with the odd numbered transmembrane α-helices, while the charged residues of these motifs form an interhelices salt bridges network that closes the cavity on the matrix side. When the internal cavity is open towards the cytosol, the transporter is in the cytoplasmic state (c-state) conformation

Table 1: SLC25 transporters known substrates, based on biochemical studies.

Approved symbol	Transported substrates	References
SLC25A1	Citrate, isocitrate, malate, phosphoenolpyruvate, and *cis*-aconitate.	[2, 4, 5]
SLC25A2	Histidine, homoarginine, monomethylarginine, and asymmetric dimethylarginine (ADMA).	[6]
SLC25A3	Phosphate, H^+, OH^-, copper.	[7, 8]
SLC25A4	adenosine triphosphate (ATP), adenosine diphosphate (ADP), H^+.	[9, 10]
SLC25A5	ATP, ADP.	[10]
SLC25A6	ATP, ADP.	[11]
UCP1 (SLC25A7)	H^+.	[12]
UCP2 (SLC25A8)	Fatty acids, H^+, malate, oxaloacetate, aspartate, malonate, sulfate, and phosphate.	[13, 14]
UCP3 (SLC25A9)	H^+.	[15]
SLC25A10	Malonate, malate, succinate, phosphate, sulfate, sulfite, thiosulfate, and glutathione.	[16–18]
SLC25A11	Oxoglutarate, malate, oxaloacetate, and glutathione.	[18–20]
SLC25A12	Glutamate, H^+, aspartate.	[21]
SLC25A13	Glutamate, H^+, aspartate.	[22]
SLC25A14 (UCP5)	Sulfate, sulfite, thiosulfate, phosphate, and dicarboxylates.	[23]
SLC25A15	Ornithine, lysine, arginine, and citrulline.	[24]
SLC25A17	Coenzyme A (CoA), flavin adenine dinucleotide (FAD), flavin mononucleotide (FMN), adenosine monophosphate (AMP), nicotinamide adenine dinucleotide (NAD^+), adenosine 3′,5′-diphosphate (PAP), ADP.	[25]
SLC25A18	Glutamate, H^+.	[26]
SLC25A19	Thiamine pyrophosphate.	[27]
SLC25A20	Carnitine, acylcarnitine.	[28]
SLC25A21	2-oxoadipate, 2-oxoglutarate, adipate, glutarate, pimelate, 2-oxopimelate, 2-aminoadipate, oxaloacetate, and citrate.	[29]
SLC25A22	Glutamate, H^+.	[26]
SLC25A23	ATP, ATP-Mg, ADP, AMP, and phosphate.	[30]
SLC25A24	ATP, ATP-Mg, ADP, AMP, and phosphate.	[30]
SLC25A26	S-adenosylmethionine.	[31]
SLC25A27 (UCP4)	H^+.	[32]
SLC25A28	Fe.	[33]
SLC25A29	Arginine, lysine, homoarginine, methylarginine, ornithine, and histidine.	[34]
SLC25A30 (UCP6)	Sulfate, sulfite, thiosulfate, phosphate, and dicarboxylates.	[23]
SLC25A31	ADP, ATP.	[35]
SLC25A32	Folate.	[36, 37]
SLC25A33	Uracil, thymine, guanine, and cytosine (deoxy)nucleoside di- and triphosphates.	[38]
SLC25A36	Uracil, thymine, guanine, and cytosine (deoxy)nucleoside di- and triphosphates.	[38]
SLC25A37	Fe.	[33]
SLC25A38	Glycine.	[39]
SLC25A41	ATP-Mg, phosphate.	[40]
SLC25A42	Coenzyme A, dephospho-CoA, ADP, and adenosine 3′,5′-diphosphate.	[41]
SLC25A44	Valine, leucine, and isoleucine.	[42]
SLC25A47	H^+.	[43]
SLC25A51	NAD^+.	[44]
SLC25A52	NAD^+.	[44]

[45]. On the contrary, the charged residues of another motif [FY][DE]xx[RK] are responsible for a salt bridges network on the "cytoplasmic" side of the protein. It is assumed that, during a catalytic transport cycle, the alternating formation of the above salt bridges networks determines the MCs' transition from the c-state to a state with the cavity open to the matrix (the m-state). Therefore the central cavity is alternatively accessible to the substrate from the intermembrane space or the matrix (Figure 1) [45].

Mutations, insertions, and deletions in the sequence of these transporters often cause numerous diseases affecting the metabolism or the energy production of the mitochondria (Table 2) [46]. Most of the missense mutations detected in patients suffering from MCs related diseases correspond to those regions of the transporters that are vital for their function [47]. For example, it is essential for the proper functioning of the transporter that no mutations occur at the substrate binding site or near the matrix/cytosolic gate [1]. On the other hand, almost all positions corresponding to residues in contact with the lipid bilayer, as well as most of those participating in inter-helices interactions, tolerate substitution with cysteine or alanine [1].

The study of membrane proteins through experimental approaches can be nontrivial. In this regard, given the recent rise in terms of computational power and the development of newer and more efficient techniques, *in silico* studies can help to understand experimental observations or propose new mechanistic theories. Here, computational analyses of the SLC25 family members are reviewed. Furthermore, new *in silico* approaches are also discussed, in order to provide a future perspective on the potential application of innovative simulation techniques to the study of this family of transporters.

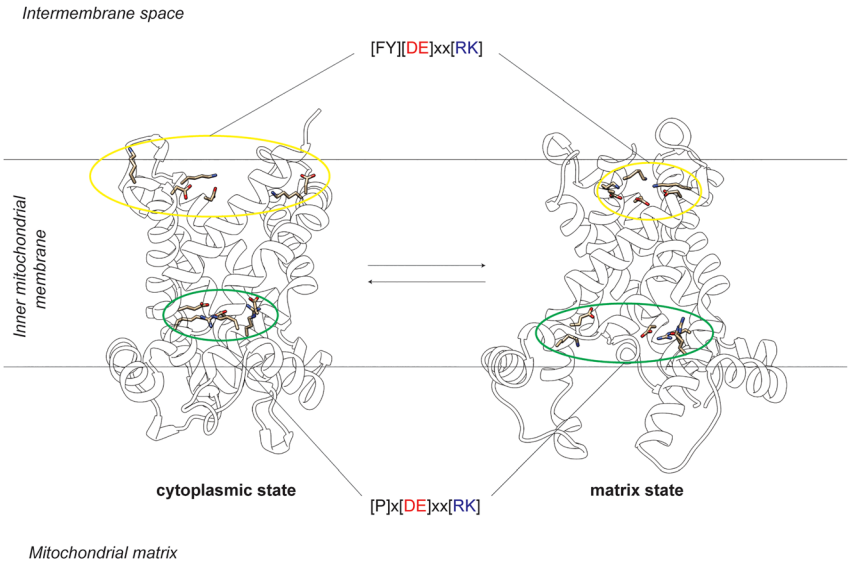

Figure 1: Representation of the cytoplasmic and matrix state of the mitochondrial carriers.
For the cytoplasmic state, the bovine ATP/ADP carrier structure (PDB ID: 1OKC) is depicted [3]; for the matrix state, the *Thermothelomyces thermophilus* ATP/ADP carrier structure (PDB ID: 6GCI) is shown [85]. Residues belonging to the matrix motif [P]x[DE]xx[RK] and involved in the matrix network salt bridges are shown as sticks and highlighted with green circles; residues belonging to the cytoplasmic motif [FY]x[DE]xx[RK] and involved in the cytoplasmic network salt bridges are shown as sticks and highlighted with yellow circles. This figure and the following ones have been drawn using UCSF Chimera molecular graphics software [177].

Computational methods for membrane proteins analysis

In the absence of experimental data, the amino acid sequence of a protein represents the starting point for analyses aimed at understanding its structure and function. Multiple sequence alignments (MSAs) of protein sequences (e.g., proteins of a given family) can help to identify conserved motifs important for molecular function, or they could highlight critical differences due to divergence in the mechanism of action or substrate specificity. In the case of membrane proteins, the sequence can also tell us how and how many times the protein backbone crosses the bilayer membrane. Several web-servers, such as TOPCONS [48], are able to predict the topology of the protein and the presence of signal peptides, allowing to better understand the spatial organization of the protein's residues. Obviously, atomic coordinates are far more useful but often really hard to obtain.

The huge amount of data derived from annotated protein sequences and structures are now important resources used to model with great accuracy the three-dimensional structure of proteins not yet solved. These approaches are divided in comparative (by homology) modeling and template-free modeling. While the first category is based on the sequence similarity between two proteins (for one of which the three-dimensional structure is known), the second can be used to build a protein's structural model from scratch. The most used comparative modeling software is MODELLER [49], where the choice of one or more suitable templates is crucial for the production of reliable results. The template structure should display at least a 30% sequence identity with the target (the protein to be modeled) and the resolution should not be above 3.5 Å [50, 51]. Historically, the I-TASSER software was the most used one for template-free modeling, this being one of the best web servers for modeling in terms of accuracy and performance [52, 53]. However, machine learning and deep learning algorithms have recently been used, which allow to achieve results never seen before (for further details about these modeling techniques see Section Structural modeling) [50]. Both the comparative and the template-free approaches resulted to be valid also for transmembrane proteins.

Once the structure is available, molecular dynamics (MD) simulations can be performed; allowing the system to explore several configurations by solving Newton's laws of motion according to interatomic forces calculated using a molecular force field [54]. With this technique, it is possible to analyze details of the conformational landscape of macromolecules that cannot be easily studied with wet lab experiments. In order to simulate membrane proteins, these must be embedded in a membrane bilayer that mimics their real molecular environment. The web-server CHARMM-GUI significantly helps users to accomplish such a task and it provides a large amount of different lipid types to build realistic biological membranes [55]. An extensive description about the setup of membrane proteins simulations can be found here [56, 57]. However, biologically relevant rare events, such as ligand binding or conformational transitions, are often very difficult to sample during atomistic simulations. Thus, several additional simulation

Table 2: Diseases associated with SLC25 transporters, based on the Online Mendelian Inheritance in Man (OMIM) database annotations.

Approved symbol	Phenotype	References
SLC25A1	Combined D-2- and L-2-hydroxyglutaric aciduria	[110, 111]
	Myasthenic syndrome, congenital, 23, presynaptic	[112–114]
SLC25A3	Mitochondrial phosphate carrier deficiency	[115–117]
SLC25A4	Mitochondrial DNA depletion syndrome 12A (cardiomyopathic type) AD	[118]
	Mitochondrial DNA depletion syndrome 12B (cardiomyopathic type) AR	[119–123]
	Progressive external ophthalmoplegia with mitochondrial DNA deletions, autosomal dominant 2	[124–126]
SLC25A10	Mitochondrial DNA depletion syndrome 19*	[127]
SLC25A11	Paragangliomas 6	[128]
SLC25A12	Developmental and epileptic encephalopathy 39	[129, 130]
SLC25A13	Citrullinemia, adult-onset type II	[131–134]
	Citrullinemia, type II, neonatal-onset	[135–137]
SLC25A15	Hyperornithinemia–hyperammonemia–homocitrullinemia syndrome	[109, 138–142]
SLC25A19	Microcephaly, Amish type	[143, 144]
	Thiamine metabolism dysfunction syndrome 4 (progressive polyneuropathy type)	[144]
SLC25A20	Carnitine–acylcarnitine translocase deficiency	[145–152]
SLC25A21	Mitochondrial DNA depletion syndrome 18*	[153]
SLC25A22	Developmental and epileptic encephalopathy 3	[154–156]
SLC25A24	Fontaine progeroid syndrome	[157–162]
SLC25A26	Combined oxidative phosphorylation deficiency 28	[163]
SLC25A32	Exercise intolerance, riboflavin-responsive*	[164]
SLC25A38	Anemia, sideroblastic, 2, pyridoxine-refractory	[165]
SLC25A42	Metabolic crises, recurrent, with variable encephalomyopathic features and neurologic regression	[166–168]
SLC25A46	Neuropathy, hereditary motor and sensory, type VIB	[169–172]
UCP2	Obesity, susceptibility to, BMIQ4**	[173, 174]
UCP3	Obesity, severe, and type II diabetes**	[175, 176]

*Provisional phenotype–gene relationship. **Susceptibility.

methods are being developed and applied. These can be divided in four groups: methods that take advantage of the thermal energy and fluctuations, such as replica exchange molecular dynamics (REMD) [58]; techniques that need different conformations of the protein in order to identify a minimum free energy path between them (e.g., milestoning [58]); other techniques that also exploit the end-point states, aiming to find a free energy difference between them [59] (in general, these are more suitable for small perturbations such as ligand binding or single point mutations); and finally, methods that apply a bias potential on a set of collective variables (CVs) (e.g., dihedral angles, distances, etc.) responsible for the slowest degrees of freedom of the system, allowing the system to overcome free energy barriers. This last group includes methods such as metadynamics [60] or adaptive biasing force [61]. The above described classification concerning the use of advanced MD sampling techniques for the study of membrane proteins is thoroughly reviewed in the work of Harpole and Delemotte [62].

Computational studies of the SLC25 protein family members

In this section, an historical perspective on the computational studies of the SLC25 protein family members is reported.

Comparative sequence/structure analyses

The first hypothesis of a common substrate binding site in MCF was formulated by Robinson and Kunji, combining experimental evidence, and computational analyses [63]. This study was conducted on the *Saccharomyces cerevisiae* MCs, as 19 of them had been already characterized at that time. In detail, these were classified into three major subfamilies, based on the functional groups of the experimentally identified substrates: keto acids carriers, amino acids carriers, and carriers of adenine-containing substrates. The MSA alone was not sufficient to assign a function to several residues identified by evolutionary conservation. For this reason, comparative structural models of the carriers (in the c-state) were built, using the structure of the mitochondrial bovine ADP/ATP carrier (bAAC, Protein Data Bank (PDB) ID: 1OKC [3]) as template. Then, the distances between the functional groups of each substrate were used to obtain positional and chemical constraints for the identification of potential binding residues.

Using this approach, some conserved residues, located in the even numbered transmembrane helices (H2, H4, and H6) of the three domains, resulted to have important correlations within their subfamilies (Figure 2).

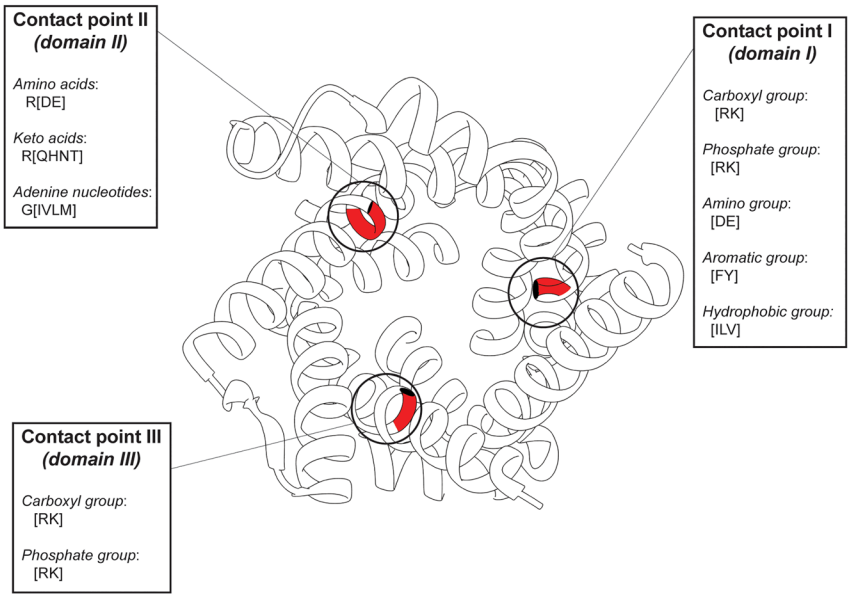

Figure 2: Schematic representation of the three contact points.
The three contact points are highlighted in red and circled, using the bovine ATP/ADP carrier structure (PDB ID: 1OKC) as reference [3]. For each contact point, a list of the corresponding residues involved in the recognition of particular ligand moieties, depending on the ligand subclass, are reported.

The residues in the first domain, collectively identified as "contact point I", were found out to discriminate between different substrates of the same class (e.g., different amino acids): basic residues [RK] are involved in carboxyl or phosphate groups recognition, acidic residues [DE] stabilize substrates' basic amino groups, aromatic residues [FY] interact with aromatic moieties and hydrophobic amino acids [ILV] are needed to form Van der Waals interactions with hydrophobic portions of the ligands.

On the contrary, the residues at the second domain, identified as "contact point II", were predicted to distinguish between different substrates classes: in the amino acid subfamily, the motif R[DE] is able to recognize the amine ($-NH_3^+$) and carboxyl ($-COO^-$) functional groups of the transported molecule; in the keto acid subfamily, the motif R[QHNT] interacts with the negatively charged keto group; and in the adenine nucleotide subfamily, the hydrophobic motif G[IVLM] recognizes the adenine moiety of the substrate.

Finally, the residues (generally R or K) located at the third domain ("contact point III") are able to recognize carboxyl or phosphate groups, stabilizing the substrate binding [63, 64]. The region of the protein in which all these contact points are located was defined as the common substrate binding site.

In a following work [45], sequence-based analyses of the 3-fold pseudo-symmetrical repeats showed that the subfamily's conserved asymmetric residues were all located in a central region of the transporters, colocalized with the previously described common substrate binding site. The symmetry analyses also suggested a 3-fold mechanism in which the transition, c- to m-state, occurs with a symmetric rotatory movement of the six α-helices.

Molecular dynamics and enhanced sampling simulations

Around the same years, there were also several attempts to analyze the transport process of MCs, exploiting computational techniques such as MD. In 2006, the first *in silico* study of the bAAC (PDB ID: 1OKC [3]), was published [65]. A MD simulation of the transporter, inserted in a palmitoyl-oleoyl-phosphatidyl-choline (POPC) bilayer membrane, allowed hypothesizing the potential role of the α-helices during the conformational changes. Notwithstanding the relatively short length of the simulation (20 ns in total), due to the limited computational resources available at that time, flexibility of the odd-numbered helices kink was pointed out through fluctuation and geometrical analyses. Three proline residues (Pro27, Pro132 and Pro229), of the conserved motif Px[DE]xx[RK], were suggested to function as hinges, critical for the movement of the helices during the transition from the c- to the m-state. Moreover, significant variations were found for the rotation angles of the even-numbered helices, and for the salt bridges connecting the transmembrane helices.

In 2008, the role of the electrostatic potential in driving the translocation of the substrate, in the AAC carrier, was investigated [66, 67]. Two papers were published, in both of which unbiased and biased MD simulations of the crystal structure of the AAC were carried out, in the presence and absence of the transported solutes ADP and/or ATP. Although in the two studies different strategies and different biased methodologies were employed, these obtained common results, pointing to a crucial role of the

protein-generated electrostatic potential in attracting the negatively charged nucleotide ADP toward the bottom of the transporter. In particular, both studies identified a common interaction of the diphosphate moiety of the substrate with residues Lys22, Arg79, and Arg279; these interactions were responsible for the disruption of the matrix network salt bridges, suggesting a possible mechanism for the conformational transition.

Eight years later, due to the advances in the computational field, atomistic simulations were able to capture and describe the transition from the c- to the m-state of the AAC [68]. The structure of the human AAC was built by homology modeling using as a template the crystal structure of bAAC [3]. A biased MD approach, the well-tempered metadynamics with multiple interacting walkers [69, 70], was used to predict the structural changes of the transporter linked to changes in free energy. The gyration radii (R_g) of three crucial regions were used as collective variables (CV); these were calculated considering the residues involved in the cytoplasmic network and aromatic gate (R_g c-gate), the substrate binding site residues (R_g center) and the matrix network residues together with the closest Pro and Gly residues (R_g m-gate). Two free energy minima were identified at the extreme values of the R_g c-gate and R_g m-gate, corresponding to the c-state and m-state conformations of the protein. Between the two minima, another free energy basin resulted to be associated with an intermediate conformation, where both the c- and m-networks are in a more closed configuration. The transition from the c- to the m-state was characterized by an activation barrier, which was reduced by the binding of ATP or ADP. Of note, the free energy minimum of the intermediate-state was deeper with the inactive nucleotides (i.e. adenosine monophosphate [AMP], guanosine triphosphate [GTP], guanosine diphosphate [GDP], and guanosine monophosphate [GMP]), preventing the conformational transition.

At the same time, a Markov model of the molecular kinetics [71], describing the stochastic motion of this carrier, was published [72]. This model, fitted on experimental data, confirmed that cytoplasmic and matrix networks have crucial roles for the conformational changes of the transporter. In particular, when the energy values of these networks are similar to each other and to the substrate binding energy, the energy barrier is minimized and the transport flow is maximized. Thus, the optimal binding of the substrate to the intermediate conformation would be responsible for the reduction of the energy barrier between c- and m-conformations.

A further study, aimed at describing the conformational transition, was carried out using a different biased MD method, called Linear Response Path Following (LRPF), which allows simulating large structural changes without knowledge of the target conformation [73, 74]. In the c- to the m-state transition, packing of the cytoplasmic network residues was observed, with a large asymmetric movement of the first domain (H1–h12–H2). This was characterized by a disruption of the salt bridge between Glu29 and Arg279, whose formation had been observed by Wang and collaborators in the simulations of the translocation of ADP [66].

Recently, an extensive unbiased MD simulation (three independent 3 μs trajectories) showed highly asymmetric interactions between the residues of the matrix network in the apo c-state of AAC [75]. In particular, a Glu29–Arg279 interaction was observed, supporting the hypothesis that this salt bridge is critical for the conformational transition. Moreover, Arg30, Arg139 and Arg236 were suggested to be responsible for the stabilization of the odd-numbered helices, through the interaction with the negative electric dipole on the C-terminal ends of these helices.

Cardiolipin–AAC interactions

Noteworthy, none of the above-mentioned studies used a bilayer membrane mimicking the inner mitochondrial membrane (IMM), where SLC25 members reside. All the systems were built homogeneously using only POPC. Instead, the IMM is made up by a mix of phospholipids, the most abundant being phosphatidylcholine (PC), phosphatidylethanolamine (PE), and cardiolipin (CL) [76]. The latter is a peculiar component of this membrane with one or two negative charges, which was experimentally described to interact with and regulate the AAC transporter [77, 78].

For this reason, several groups tried to analyze the characteristics of this interaction *in silico*.

Coarse-grained (CG) and atomistic simulations were applied to investigate the binding of CL to bovine and yeast AAC (PDB ID: 1OKC [3]; PDB ID: 4C9G [79]) and UCP2 (uncoupling protein 2; PDB ID: 2LCK [80]) [81]. CL molecules were predicted to bind at three different sites with the phosphate groups inserted in the cavities produced by the three short α-helices (h12, h34, and h56), in correspondence of the highly conserved [YWF][RK]G and [YF]xG motifs, consistent with what had been observed experimentally [3, 82].

These findings were confirmed by Duncan and colleagues [83], who also analysed lipid–AAC interactions performing multiscale simulations (both CG and atomistic). Of note, they observed that the residence time of CL was very peculiar, as it was significantly higher than the residence time of PC and PE.

Moreover, the simulations performed by Yi and collaborators showed that the conserved CL-binding motifs [YWF][RK]G and [YF]xG were organized in β-turn structures, responsible for the interaction and stabilization of the three Pro kink regions, but not in a symmetric manner [75].

The same group recently reported an additional computational study of the CL–AAC binding [84], in which a long simulation (13 μs) allowed to observe a dynamic interaction in three different protein regions, previously described as binding sites. However, in one binding site the CL molecule had mostly inter-domain interactions (domain 2 and 3), while in the other two binding sites CLs mainly established intradomain interactions (domain 1 or 3). Again, these asymmetrical binding modes were consistent with their previous study [75] and it suggested a physiological relevance for the displacement of domain 1 observed in the recently solved AAC structure in the m-state [85].

These results suggest an asymmetrical behavior of the transporter, a hypothesis supported also by other MD studies [73, 86].

Future perspectives

Structural modeling

During the last years, thanks to new powerful algorithms, computational techniques for the modeling of protein structures significantly improved, as resulted also during the 13th Critical Assessment of protein Structure Prediction (CASP13), where the artificial intelligence (AI)-based method developed by DeepMind, AlphaFold, outperformed all other methods [87]. This is a co evolution based method that uses the protein's MSAs to detect the residues that co-evolve, predicting a probability distribution over the pairwise distances between the residues pairs. This can be translated into a statistical potential function and then optimized with a simple gradient descent algorithm to generate a folded protein structure [88, 89]. A similar approach was implemented in a method developed by Jinbo Xu's group, named RaptorX [90], and in a method from Baker's group, called trRosetta [91]. The big advancement in this field could clearly allow generating highly reliable structural models of MC family members whose structure is not available yet.

As an example, using the two latter methods, different conformations of bAAC and *Thermothelomyces thermophilus* AAC (TtAAC) (PDB ID: 1OKC [3]; PDB ID: 6GCI [85]), were obtained (Figure 3) (Pasquadibisceglie & Polticelli, unpublished data). In particular, compared to the experimentally solved structures, the modeled structures display lower gyration radii of the cytoplasmic network residues (using the open-source, community-developed PLUMED library [92], version 2.7 [93]), pointing out a more closed conformation of the cytoplasmic side. Conversely, compared to the experimentally solved structures, the gyration radii of the matrix networks were higher in the case of the bAAC model structure, but lower for the TtAAC model structure. This is due to the different conformations of the two crystal structures (bAAC in c-state, while TtAAC in m-state) (Table 3). Moreover, the presence of inhibitors and/or antibody fragments in the solved structures, used to block the proteins in a precise conformation, are likely to cause structural distortions, in line with what Falconi and Dehez, independently, observed [65, 67]. However, it should be noted that the two above-mentioned modeling approaches exploit the information about co evolving residues; this could result in favoring lower distances between the interacting residues of the matrix and cytoplasmic networks, thus producing intermediate-like conformations.

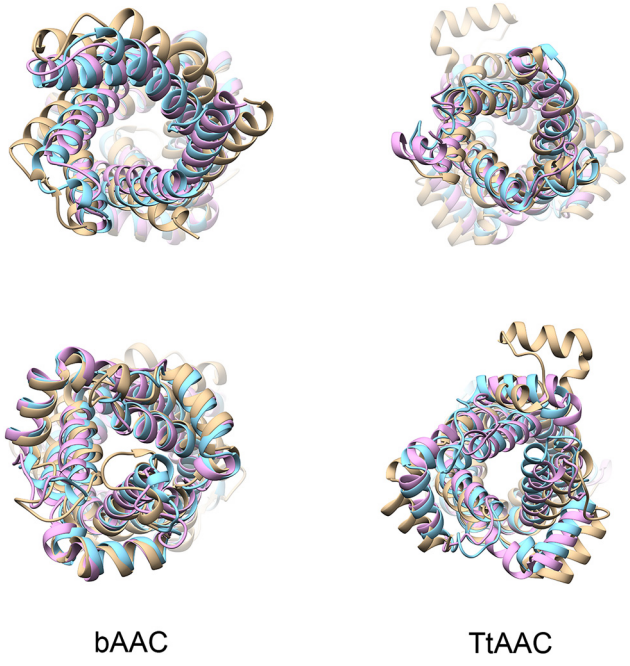

Figure 3: Superimposition of the three-dimensional structures and the molecular models of the bovine ATP/ADP carrier (bAAC), and the ATP/ADP carrier from *Thermothelomyces thermophilus* (TtAAC) [3, 80, 85]. View from the inner mitochondrial space (top), and from the matrix (bottom). The structure solved experimentally is colored in tan, the structure modelled with RaptorX in light blue [90] and the structural model produced by trRosetta in pink [91].

Table 3: Radius of gyration analysis performed on the alpha carbons of the matrix and cytoplasmic network residues.

	Cytoplasmic network	Matrix network
bAAC (1OKC)	14 Å	7.5 Å
bAAC (RaptorX)	9.5 Å	7.3 Å
bAAC (trRosetta)	8.3 Å	7.4 Å
TtAAC (6GCI)	7.9 Å	11.8 Å
TtAAC (RaptorX)	8.5 Å	7.3 Å
TtAAC (trRosetta)	7.9 Å	7.5 Å

Finally, to improve the accuracy of the model of a protein structure the refinement step is crucial. MD simulations are often used to accomplish such a task. However, it is nontrivial to consistently improve a structural model and select the conformation closer to the native state [94]. This is especially true for membrane proteins models, where the scoring function has to take into account the presence of a lipid bilayer. In this regard, refinement protocols and scoring functions developed specifically for membrane proteins [95] could improve the modeling accuracy for this class of proteins in general and for the SLC superfamily members in particular.

System setup for MD simulations

As several studies showed, CL is a crucial phospholipid for the IMM and for the MCs, affecting their dynamics [75, 77, 78, 81–84]. For this reason, MD simulations would be more accurate and reliable if the transporters were embedded in a lipid bilayer that mimics the concentration of CL and the relative asymmetric distribution, this phospholipid being predominant in the inner leaflet with respect to the outer one, in a 3:1 ratio [76, 96]. Also the fatty acids composition often does not reproduce that of a realistic IMM, characterized by a high degree of unsaturation [97, 98]. Nowadays, thanks to the great advances in the field of atomistic and CG force fields, more realistic membrane models are being used for MD simulations, trying to reproduce complex systems and interactions, and in this regard CHARMM-GUI represents a valuable resource [55, 99].

Sampling of rare events

Biological processes, such as the m- to the c-state transition or the substrate translocation, occur in the timescale of microseconds to seconds.

One solution to sample these rare events could be that of extending the simulation length, but this is not really convenient due to the effort needed in terms of computational resources. A larger time step allows extending the simulation time with a lower computational effort. This can be easily achieved using the method of hydrogen mass repartitioning (HMR), where the mass of heavy atoms is redistributed onto their bonded hydrogens, slowing their motions without introducing significant additional errors [99]. In a recent study, the use of HMR for membrane-containing systems (with CHARMM36 FF) has been extensively tested, showing negligible differences with respect to a conventional approach. However, the authors pointed out that, using the CHARMM36 lipid FF, a cutoff different from 12 Å with a force switching function starting from 8 to 10 Å could generate significant deviations on several parameters [99].

Anyhow, biologically relevant rare events are often very difficult to sample during atomistic simulations, even during microseconds-long trajectories. In this regard, two enhanced sampling strategies have been used to study the transport mechanism of the AAC, and its relative free energy landscape [68, 73]. Nevertheless, the application of new methods could better clarify several aspects of this and other systems. For example, supervised and unsupervised machine learning algorithms could be exploited for the selection of CVs, to better understand the properties of a simulated system, or to accelerate the sampling during the trajectory (i.e., enhanced sampling) [100]. Moreover, other advanced MD techniques are being developed, such as the on-the-fly probability-enhanced sampling (OPES) that avoids the sampling of unphysical states and that allows a better exploration of the free energy surface [101].

Conclusions

The studies here reviewed showed how computational approaches could suggest new hypotheses or support experimental evidences: comparative analyses identified critical residues for the substrate recognition [63, 64], further supported by MD simulations [66, 67], cocrystallized inhibitors [3] and photolabeling studies [102]. In a similar way, the salt bridges networks involved in the conformational changes were identified from comparative studies [45], crystallized structures [3, 85] and mutagenesis experiments [79], whereas MD evidenced the dynamical behavior of these interactions [66, 68, 73, 75]. Finally, several groups pointed out the relevance of cardiolipin binding through crystal structures [3, 82], phosphorous nuclear magnetic resonance (NMR) [77], and thermostability studies [103], as well as atomistic and coarse-grained simulations [81, 83, 84].

Thus, the newest modeling methods together with the most recent and powerful MD techniques will allow to study with higher accuracy the AAC transporter and all the other SLC25 family members, for which very few structural data are available in literature, suggesting and/or supporting new mechanistic hypotheses [104–109].

Acknowledgments: Not applicable.
Research funding: This research was funded by the Italian Ministry of University and Research (MIUR), grants "Dipartimenti di Eccellenza" (Legge 232/2016, Articolo 1, Comma 314–337) and PRIN (Grant No. 2017483NH8).
Author contributions: Conceptualization, A.P. and F.P.; writing – original draft preparation, A.P.; writing – review and editing, A.P. and F.P.; supervision, F.P.; project administration, F.P.; funding acquisition, F.P. All authors have read and agreed to the published version of the manuscript. All authors have accepted responsibility for the entire content of this manuscript and approved its submission.
Competing interests: The funders had no role in the design of the study; in the collection, analyses, or interpretation of data; in the writing of the manuscript, or in the decision to publish the results. The authors declare no conflict of interest.
Informed consent: Not applicable.
Ethical approval: Not applicable.

References

1. Palmieri F. Mitochondrial transporters of the SLC25 family and associated diseases: a review. J Inherit Metab Dis 2014;37:565–75.
2. Claeys D, Azzi A. Tricarboxylate carrier of bovine liver mitochondria. Purification and reconstitution. J Biol Chem 1989; 264:14627–30.
3. Pebay-Peyroula E, Dahout-Gonzalez C, Kahn R, Trézéguet V, Lauquin GJM, Brandolin G. Structure of mitochondrial ADP/ATP carrier in complex with carboxyatractyloside. Nature 2003;426: 39–44.
4. Palmieri F, Stipani I, Quagliariello E, Klingenberg M. Kinetic study of the tricarboxylate carrier in rat liver mitochondria. Eur J Biochem 1972;26:587–94.
5. Majd H, King MS, Smith AC, Kunji ERS. Pathogenic mutations of the human mitochondrial citrate carrier SLC25A1 lead to impaired citrate export required for lipid, dolichol, ubiquinone and sterol synthesis. Biochim Biophys Acta Bioenerg 2018;1859:1–7.
6. Porcelli V, Longo A, Palmieri L, Closs EI, Palmieri F. Asymmetric dimethylarginine is transported by the mitochondrial carrier SLC25A2. Amino Acids 2016;48:427–36.
7. Stappen R, Krämer R. Kinetic mechanism of phosphate/phosphate and phosphate/OH-antiports catalyzed by reconstituted phosphate carrier from beef heart mitochondria. J Biol Chem 1994; 269:11240–6.
8. Boulet A, Vest KE, Maynard MK, Gammon MG, Russell AC, Mathews AT, et al. The mammalian phosphate carrier SLC25A3 is a mitochondrial copper transporter required for cytochrome c oxidase biogenesis. J Biol Chem 2018;293:1887–96.
9. Bertholet AM, Chouchani ET, Kazak L, Angelin A, Fedorenko A, Long JZ, et al. H^+ transport is an integral function of the mitochondrial ADP/ATP carrier. Nature 2019;571:515–20.
10. Klingenberg M. The ADP and ATP transport in mitochondria and its carrier. Biochim Biophys Acta Biomembr 2008;1778: 1978–2021.
11. Stepien G, Torroni A, Chung AB, Hodge JA, Wallaces DC. Differential expression of adenine nucleotide translocator isoforms in mammalian tissues and during muscle cell differentiation. J Biol Chem 1992;267:14592–7.
12. Casteilla L, Blondel O, Klaus S, Raimbault S, Diolez P, Moreau F, et al. Stable expression of functional mitochondrial uncoupling protein in Chinese hamster ovary cells. Proc Natl Acad Sci USA 1990;87. https://doi.org/10.1073/pnas.87.13.5124.
13. Berardi MJ, Chou JJ. Fatty acid flippase activity of UCP2 is essential for its proton transport in mitochondria. Cell Metabol 2014;20:541–52.
14. Vozza A, Parisi G, De Leonardis F, Lasorsa FM, Castegna A, Amorese D, et al. UCP2 transports C4 metabolites out of mitochondria, regulating glucose and glutamine oxidation. Proc Natl Acad Sci USA 2014;111:960–5.
15. Macher G, Koehler M, Rupprecht A, Kreiter J, Hinterdorfer P, Pohl EE. Inhibition of mitochondrial UCP1 and UCP3 by purine nucleotides and phosphate. Biochim Biophys Acta Biomembr 2018;1860:664–72.
16. Palmieri F, Prezioso G, Quagliariello E, Klingenberg M. Kinetic study of the dicarboxylate carrier in rat liver mitochondria. Eur J Biochem 1971;22:66–74.
17. Crompton M, Palmieri F, Capano M, Quagliariello E. The transport of thiosulphate in rat liver mitochondria. FEBS Lett 1974;46: 247–50.
18. Chen Z, Lash LH. Evidence for mitochondrial uptake of glutathione by dicarboxylate and 2-oxoglutarate carriers. J Pharmacol Exp Therapeut 1998;285:608–18.
19. Palmieri F, Quagliariello E, Klingenberg M. Kinetics and specificity of the oxoglutarate carrier in rat-liver mitochondria. Eur J Biochem 1972;29:408–16.
20. Passarella S, Palmieri F, Quagliariello E. The transport of oxaloacetate in isolated mitochondria. Arch Biochem Biophys 1977;180:160–8.
21. LaNoue KF, Tischler ME. Electrogenic characteristics of the mitochondrial glutamate aspartate antiporter. J Biol Chem 1974; 249:7522–8.
22. Palmieri L, Pardo B, Lasorsa FM, Del Arco A, Kobayashi K, Iijima M, et al. Citrin and aralar1 are Ca^{2+}-stimulated aspartate/glutamate transporters in mitochondria. EMBO J 2001;20:5060–9.
23. Gorgoglione R, Porcelli V, Santoro A, Daddabbo L, Vozza A, Monné M, et al. The human uncoupling proteins 5 and 6 (UCP5/ SLC25A14 and UCP6/SLC25A30) transport sulfur oxyanions, phosphate and dicarboxylates. Biochim Biophys Acta Bioenerg 2019;1860:724–33.
24. Fiermonte G, Dolce V, David L, Santorelli FM, Dionisi-Vici C, Palmieri F, et al. The mitochondrial ornithine transporter: bacterial expression, reconstitution, functional characterization, and tissue distribution of two human isoforms. J Biol Chem 2003; 278:32778–83.

25. Agrimi G, Russo A, Scarcia P, Palmieri F. The human gene SLC25A17 encodes a peroxisomal transporter of coenzyme A, FAD and NAD^+. Biochem J 2012;443:241–7.
26. Fiermonte G, Palmieri L, Todisco S, Agrimi G, Palmieri F, Walker JE. Identification of the mitochondrial glutamate transporter. Bacterial expression, reconstitution, functional characterization, and tissue distribution of two human isoforms. J Biol Chem 2002; 277:19289–94.
27. Kang J, Samuels DC. The evidence that the DNC (SLC25A19) is not the mitochondrial deoxyribonucleotide carrier. Mitochondrion 2008;8:103–8.
28. Indiveri C, Iacobazzi V, Giangregorio N, Palmieri F. Bacterial overexpression, purification, and reconstitution of the carnitine/ acylcarnitine carrier from rat liver mitochondria. Biochem Biophys Res Commun 1998;249:589–94.
29. Fiermonte G, Dolce V, Palmieri L, Ventura M, Runswick MJ, Palmieri F, et al. Identification of the human mitochondrial oxodicarboxylate carrier. Bacterial expression, reconstitution, functional characterization, tissue distribution, and chromosomal location. J Biol Chem 2001;276:8225–30.
30. Fiermonte G, De Leonardis F, Todisco S, Palmieri L, Lasorsa FM, Palmieri F. Identification of the mitochondrial ATP-Mg/Pi transporter: bacterial expression, reconstitution, functional characterization, and tissue distribution. J Biol Chem 2004;279: 30722–30.
31. Agrimi G, Di Noia MA, Marobbio CMT, Fiermonte G, Lasorsa FM, Palmieri F. Identification of the human mitochondrial S-adenosylmethionine transporter: bacterial expression, reconstitution, functional characterization and tissue distribution. Bio chem J 2004;379:183–90.
32. Hoang T, Smith MD, Jelokhani-Niaraki M. Toward understanding the mechanism of ion transport activity of neuronal uncoupling proteins UCP2, UCP4, and UCP5. Biochemistry 2012;51:4004–14.
33. Paradkar PN, Zumbrennen KB, Paw BH, Ward DM, Kaplan J. Regulation of mitochondrial iron import through differential turnover of mitoferrin 1 and mitoferrin 2. Mol Cell Biol 2009;29: 1007–16.
34. Porcelli V, Fiermonte G, Longo A, Palmieri F. The human gene SLC25A29, of solute carrier family 25, encodes a mitochondrial transporter of basic amino acids. J Biol Chem 2014;289: 13374–84.
35. Dolce V, Scarcia P, Iacopetta D, Palmieri F. A fourth ADP/ATP carrier isoform in man: identification, bacterial expression, functional characterization and tissue distribution. FEBS Lett 2005;579:633–7.
36. McCarthy EA, Titus SA, Taylor SM, Jackson-Cook C, Moran RG. A mutation inactivating the mitochondrial inner membrane folate transporter creates a glycine requirement for survival of Chinese hamster cells. J Biol Chem 2004;279:33829–36.
37. Titus SA, Moran RG. Retrovirally mediated complementation of the glyB phenotype. Cloning of a human gene encoding the carrier for entry of folates into mitochondria. J Biol Chem 2000; 275:36811–7.
38. Di Noia MA, Todisco S, Cirigliano A, Rinaldi T, Agrimi G, Iacobazzi V, et al. The human SLC25A33 and SLC25A36 genes of solute carrier family 25 encode two mitochondrial pyrimidine nucleotide transporters. J Biol Chem 2014;289:33137–48.
39. Lunetti P, Damiano F, De Benedetto G, Siculella L, Pennetta A, Muto L, et al. Characterization of human and yeast mitochondrial glycine carriers with implications for heme biosynthesis and anemia. J Biol Chem 2016;291:19746–59.
40. Traba J, Satrústegui J, del Arco A. Characterization of SCaMC-3-like/slc25a41, a novel calcium-independent mitochondrial ATP-Mg/Pi carrier. Biochem J 2009;418:125–33.
41. Fiermonte G, Paradies E, Todisco S, Marobbio CMT, Palmieri F. A novel member of solute carrier family 25 (SLC25A42) is a transporter of coenzyme A and adenosine 3′,5′-diphosphate in human mitochondria. J Biol Chem 2009;284:18152–9.
42. Yoneshiro T, Wang Q, Tajima K, Matsushita M, Maki H, Igarashi K, et al. BCAA catabolism in brown fat controls energy homeostasis through SLC25A44. Nature 2019;572:614–9.
43. Jin X, Yang YD, Chen K, Lv ZY, Zheng L, Liu YP, et al. HDMCP uncouples yeast mitochondrial respiration and alleviates steatosis in L02 and hepG2 cells by decreasing ATP and H_2O_2 levels: a novel mechanism for NAFLD. J Hepatol 2009;50: 1019–28.
44. Luongo TS, Eller JM, Lu MJ, Niere M, Raith F, Perry C, et al. SLC25A51 is a mammalian mitochondrial NAD^+ transporter. Nature 2020;588:174–9.
45. Robinson AJ, Overy C, Kunji ERS. The mechanism of transport by mitochondrial carriers based on analysis of symmetry. Proc Natl Acad Sci USA 2008;105:17766–71.
46. Palmieri F, Scarcia P, Monné M. Diseases caused by mutations in mitochondrial carrier genes SLC25: a review. Biomolecules 2020; 10:655.
47. Palmieri F, Monné M. Discoveries, metabolic roles and diseases of mitochondrial carriers: a review. Biochim Biophys Acta Mol Cell Res 2016;1863:2362–78.
48. Tsirigos KD, Peters C, Shu N, Käll L, Elofsson A. The TOPCONS web server for consensus prediction of membrane protein topology and signal peptides. Nucleic Acids Res 2015;43:W401–7.
49. Webb B, Sali A. Comparative protein structure modeling using MODELLER. Curr Protoc Bioinf 2016;54. 5.6.1–37.
50. Croll TI, Sammito MD, Kryshtafovych A, Read RJ. Evaluation of template-based modeling in CASP13. Proteins Struct Funct Bioinf 2019;87:1113–27.
51. Baker D, Sali A. Protein structure prediction and structural genomics. Science 2001;294:93–6.
52. Abriata LA, Tamò GE, Monastyrskyy B, Kryshtafovych A, Dal Peraro M. Assessment of hard target modeling in CASP12 reveals an emerging role of alignment-based contact prediction methods. Proteins Struct Funct Bioinf 2018;86:97–112.
53. Yang J, Zhang Y. I-TASSER server: new development for protein structure and function predictions. Nucleic Acids Res 2015;43: W174–81.
54. Karplus M, McCammon JA. Molecular dynamics simulations of biomolecules. Nat Struct Biol 2002;9:646–52.
55. Wu EL, Cheng X, Jo S, Rui H, Song KC, Dávila-Contreras EM, et al. CHARMM-GUI membrane builder toward realistic biological membrane simulations. J Comput Chem 2014;35:1997–2004.
56. Kandt C, Ash WL, Peter Tieleman D. Setting up and running molecular dynamics simulations of membrane proteins. Methods 2007;41:475–88.
57. Jefferies D, Khalid S. Atomistic and coarse-grained simulations of membrane proteins: a practical guide. Methods 2020;185:15–27.
58. Sugita Y, Okamoto Y. Replica-exchange molecular dynamics method for protein folding. Chem Phys Lett 1999;314:141–51.

59. Seeliger D, de Groot BL. Protein thermostability calculations using alchemical free energy simulations. Bio phys J 2010;98: 2309–16.
60. Laio A, Parrinello M. Escaping free-energy minima. Proc Natl Acad Sci USA 2002;99:12562–6.
61. Darve E, Rodríguez-Gómez D, Pohorille A. Adaptive biasing force method for scalar and vector free energy calculations. J Chem Phys 2008;128:144120.
62. Harpole TJ, Delemotte L. Conformational landscapes of membrane proteins delineated by enhanced sampling molecular dynamics simulations. Biochim Biophys Acta Biomembr 2018; 1860:909–26.
63. Robinson AJ, Kunji ERS. Mitochondrial carriers in the cytoplasmic state have a common substrate binding site. Proc Natl Acad Sci USA 2006;103:2617–22.
64. Kunji ERS, Robinson AJ. The conserved substrate binding site of mitochondrial carriers. Biochim Biophys Acta Bioenerg 2006; 1757:1237–48.
65. Falconi M, Chillemi G, Di Marino D, D'Annessa I, Morozzo della Rocca B, Palmieri L, et al. Structural dynamics of the mitochondrial ADP/ATP carrier revealed by molecular dynamics simulation studies. Proteins Struct Funct Bioinf 2006; 65:681–91.
66. Wang Y, Tajkhorshid E. Electrostatic funneling of substrate in mitochondrial inner membrane carriers. Proc Natl Acad Sci USA 2008;105:9598–603.
67. Dehez F, Pebay-Peyroula E, Chipot C. Binding of ADP in the mitochondrial ADP/ATP carrier is driven by an electrostatic funnel. J Am Chem Soc 2008;130:12725–33.
68. Pietropaolo A, Pierri CL, Palmieri F, Klingenberg M. The switching mechanism of the mitochondrial ADP/ATP carrier explored by free-energy landscapes. Biochim Biophys Acta Bioenerg 2016; 1857:772–81.
69. Barducci A, Bussi G, Parrinello M. Well-tempered metadynamics: a smoothly converging and tunable free-energy method. Phys Rev Lett 2008;100:020603.
70. Raiteri P, Laio A, Gervasio FL, Micheletti C, Parrinello M. Efficient reconstruction of complex free energy landscapes by multiple walkers metadynamics. J Phys Chem B 2006;110:3533–9.
71. Prinz JH, Wu H, Sarich M, Keller B, Senne M, Held M, et al. Markov models of molecular kinetics: generation and validation. J Chem Phys 2011;134:174105.
72. Springett R, King MS, Crichton PG, Kunji ERS. Modelling the free energy profile of the mitochondrial ADP/ATP carrier. Biochim Biophys Acta Bioenerg 2017;1858:906–14.
73. Tamura K, Hayashi S. Atomistic modeling of alternating access of a mitochondrial ADP/ATP membrane transporter with molecular simulations. PloS One 2017;12:e0181489.
74. Tamura K, Hayashi S. Linear response path following: a molecular dynamics method to simulate global conformational changes of protein upon ligand binding. J Chem Theor Comput 2015;11: 2900–17.
75. Yi Q, Li Q, Yao S, Chen Y, Guan MX, Cang X. Molecular dynamics simulations on apo ADP/ATP carrier shed new lights on the featured motif of the mitochondrial carriers. Mitochondrion 2019; 47:94–102.
76. Horvath SE, Daum G. Lipids of mitochondria. Prog Lipid Res 2013; 52:590–614.
77. Beyer K, Klingenberg M. ADP/ATP carrier protein from beef heart mitochondria has high amounts of tightly bound cardiolipin, as revealed by 31P nuclear magnetic resonance. Biochemistry 1985; 24:3821–6.
78. Klingenberg M. Cardiolipin and mitochondrial carriers. Biochim Biophys Acta Biomembr 2009;1788:2048–58.
79. Ruprecht JJ, Hellawell AM, Harding M, Crichton PG, McCoy AJ, Kunji ERS. Structures of yeast mitochondrial ADP/ATP carriers support a domain-based alternating-access transport mechanism. Proc Natl Acad Sci USA 2014;111:E426–34.
80. Berardi MJ, Shih WM, Harrison SC, Chou JJ. Mitochondrial uncoupling protein 2 structure determined by NMR molecular fragment searching. Nature 2011;476:109–14.
81. Hedger G, Rouse SL, Domański J, Chavent M, Koldsø H, Sansom MSP. Lipid-loving ANTs: molecular simulations of cardiolipin interactions and the organization of the adenine nucleotide translocase in model mitochondrial membranes. Biochemistry 2016;55:6238–49.
82. Nury H, Dahout-Gonzalez C, Trézéguet V, Lauquin G, Brandolin G, Pebay-Peyroula E. Structural basis for lipid-mediated interactions between mitochondrial ADP/ATP carrier monomers. FEBS Lett 2005;579:6031–6.
83. Duncan AL, Ruprecht JJ, Kunji ERS, Robinson AJ. Cardiolipin dynamics and binding to conserved residues in the mitochondrial ADP/ATP carrier. Biochim Biophys Acta Biomembr 2018;1860: 1035–45.
84. Mao X, Yao S, Yi Q, Xu ZM, Cang X. Function-related asymmetry of the specific cardiolipin binding sites on the mitochondrial ADP/ ATP carrier. Biochim Biophys Acta Biomembr 2021;1863:183466 https://doi.org/10.1016/j.bbamem.2020.183466.
85. Ruprecht JJ, King MS, Zögg T, Aleksandrova AA, Pardon E, Crichton PG, et al. The molecular mechanism of transport by the mitochondrial ADP/ATP carrier. Cell 2019;176:435–47.e15.
86. Škulj S, Brkljača Z, Vazdar M. Molecular dynamics simulations of the elusive matrix-open state of mitochondrial ADP/ATP carrier. Isr J Chem 2020;60:735–43.
87. Abriata LA, Tamò GE, Dal Peraro M. A further leap of improvement in tertiary structure prediction in CASP13 prompts new routes for future assessments. Proteins Struct Funct Bioinf 2019;87: 1100–12.
88. Senior AW, Evans R, Jumper J, Kirkpatrick J, Sifre L, Green T, et al. Protein structure prediction using multiple deep neural networks in the 13th Critical Assessment of Protein Structure Prediction (CASP13). Proteins Struct Funct Bioinf 2019;87:1141–8.
89. Senior AW, Evans R, Jumper J, Kirkpatrick J, Sifre L, Green T, et al. Improved protein structure prediction using potentials from deep learning. Nature 2020;577:706–10.
90. Xu J. Distance-based protein folding powered by deep learning. Proc Natl Acad Sci USA 2019;116:16856–65.
91. Yang J, Anishchenko I, Park H, Peng Z, Ovchinnikov S, Baker D. Improved protein structure prediction using predicted interresidue orientations. Proc Natl Acad Sci USA 2020;117: 1496–503.
92. Bonomi M, Bussi G, Camilloni C, Tribello GA, Banáš P, Barducci A, et al. Promoting transparency and reproducibility in enhanced molecular simulations. Nat Methods 2019;16:670–3.
93. Tribello GA, Bonomi M, Branduardi D, Camilloni C, Bussi G. PLUMED 2: new feathers for an old bird. Comput Phys Commun 2014;185:604–13.
94. Heo L, Feig M. Experimental accuracy in protein structure refinement via molecular dynamics simulations. Proc Natl Acad Sci USA 2018;115:13276–81.

95. Dutagaci B, Heo L, Feig M. Structure refinement of membrane proteins via molecular dynamics simulations. Proteins Struct Funct Bioinf 2018;86:738–50.
96. Krebs JJR, Hauser H, Carafoli E. Asymmetric distribution of phospholipids in the inner membrane of beef heart mitochondria. J Biol Chem 1979;254:5308–16.
97. Comte J, Maïsterrena B, Gautheron DC. Lipid composition and protein profiles of outer and inner membranes from pig heart mitochondria. Comparison with microsomes. Biochim Biophys Acta Biomembr 1976;419:271–84.
98. Colbeau A, Nachbaur J, Vignais PM. Enzymac characterization and lipid composition of rat liver subcellular membranes. Biochim Biophys Acta Biomembr 1971;249:462–92.
99. Marrink SJ, Corradi V, Souza PCT, Ingólfsson HI, Tieleman DP, Sansom MSP. Computational modeling of realistic cell membranes. Chem Rev 2019;119:6184–226.
100. Fleetwood O, Kasimova MA, Westerlund AM, Delemotte L. Molecular insights from conformational ensembles via machine learning. Biophys J 2020;118:765–80.
101. Invernizzi M, Parrinello M. Rethinking metadynamics: from bias potentials to probability distributions. J Phys Chem Lett 2020;11: 2731–6.
102. Dalbon P, Brandolin G, Boulay F, Hoppe J, Vignais PV. Mapping of the nucleotide-binding sites in the ADP/ATP carrier of beef heart mitochondria by photolabeling with 2-azido[α-32p]adenosine diphosphate. Biochemistry 1988;27:5141–9.
103. Crichton PG, Lee Y, Ruprecht JJ, Cerson E, Thangaratnarajah C, King MS, et al. Trends in thermostability provide information on the nature of substrate, inhibitor, and lipid interactions with mitochondrial carriers. J Biol Chem 2015;290:8206–17.
104. Giangregorio N, Tonazzi A, Console L, Prejanò M, Marino T, Russo N, et al. Effect of copper on the mitochondrial carnitine/ acylcarnitine carrier via interaction with Cys136 and Cys155. Possible implications in pathophysiology. Molecules 2020;25: 820.
105. Zoonens M, Comer J, Masscheleyn S, Pebay-Peyroula E, Chipot C, Miroux B, et al. Dangerous liaisons between detergents and membrane proteins. the case of mitochondrial uncoupling protein 2. J Am Chem Soc 2013;135:15174–82.
106. Hoang T, Smith MD, Jelokhani-Niaraki M. Toward understanding the mechanism of ion transport activity of neuronal uncoupling proteins UCP2, UCP4, and UCP5. Biochemistry 2012;51: 4004–14.
107. Sun J, Aluvila S, Kotaria R, Mayor JA, Walters DE, Kaplan RS. Mitochondrial and plasma membrane citrate transporters: discovery of selective inhibitors and application to structure/ function analysis. Mol Cell Pharmacol 2010;2:101–10.
108. Monné M, Miniero DV, Daddabbo L, Robinson AJ, Kunji ERS, Palmieri F. Substrate specificity of the two mitochondrial ornithine carriers can be swapped by single mutation in substrate binding site. J Biol Chem 2012;287:7925–34.
109. Tessa A, Fiermonte G, Dionisi-Vici C, Paradies E, Baumgartner MR, Chien Y-H, et al. Identification of novel mutations in the *SLC25A15* gene in hyperornithinemia-hyperammonemia-homocitrullinuria (HHH) syndrome: a clinical, molecular, and functional study. Hum Mutat 2009;30:741–8.
110. Nota B, Struys EA, Pop A, Jansen EE, Fernandez Ojeda MR, Kanhai WA, et al. Deficiency in SLC25A1, encoding the mitochondrial citrate carrier, causes combined D-2- and L-2-hydroxyglutaric aciduria. Am J Hum Genet 2013;92:627–31.
111. Edvardson S, Porcelli V, Jalas C, Soiferman D, Kellner Y, Shaag A, et al. Agenesis of corpus callosum and optic nerve hypoplasia due to mutations in SLC25A1 encoding the mitochondrial citrate transporter. J Med Genet 2013;50:240–5.
112. Al-Futaisi A, Ahmad F, Al-Kasbi G, Al-Thihli K, Koul R, Al-Maawali A. Missense mutations in *SLC25A1* are associated with congenital myasthenic syndrome type 23. Clin Genet 2020;97: 666–7.
113. Chaouch A, Porcelli V, Cox D, Edvardson S, Scarcia P, De Grassi A, et al. Mutations in the mitochondrial citrate carrier SLC25A1 are associated with impaired neuromuscular transmission. J Neuromuscul Dis 2014;1:75–90.
114. Balaraju S, Töpf A, McMacken G, Kumar VP, Pechmann A, Roper H, et al. Congenital myasthenic syndrome with mild intellectual disability caused by a recurrent SLC25A1 variant. Eur J Hum Genet 2020;28:373–7.
115. Bhoj EJ, Li M, Ahrens-Nicklas R, Pyle LC, Wang J, Zhang VW, et al. Pathologic variants of the mitochondrial phosphate carrier SLC25A3: two new patients and expansion of the cardiomyopathy/skeletal myopathy phenotype with and without lactic acidosis. JIMD Rep 2015;19:59–66. Springer.
116. Mayr JA, Merkel O, Kohlwein SD, Gebhardt BR, Böhles H, Fötschl U, et al. Mitochondrial phosphate-carrier deficiency: a novel disorder of oxidative phosphorylation. Am J Hum Genet 2007; 80:478–84.
117. Mayr JA, Zimmermann FA, Horváth R, Schneider HC, Schoser B, Holinski-Feder E, et al. Deficiency of the mitochondrial phosphate carrier presenting as myopathy and cardiomyopathy in a family with three affected children. Neuromuscul Disord 2011;21:803–8.
118. Thompson K, Majd H, Dallabona C, Reinson K, King MS, Alston CL, et al. Recurrent de novo dominant mutations in SLC25A4 cause severe early-onset mitochondrial disease and loss of mitochondrial DNA copy number. Am J Hum Genet 2016;99: 860–76.
119. Bakker HD, Scholte HR, Van den Bogert C, Jeneson JAL, Ruitenbeek W, Wanders RJA, et al. Adenine nucleotide translocator deficiency in muscle: potential therapeutic value of vitamin E. J Inherit Metab Dis 1993;16:548–52.
120. Bakker HD, Scholte HR, Van Den Bogert C, Ruitenbeer W, Jeneson JAL, Wanders RJA, et al. Deficiency of the adenine nucleotide translocator in muscle of a patient with myopathy and lactic acidosis: a new mitochondrial defect. Pediatr Res 1993;33: 412–7.
121. Echaniz-Laguna A, Chassagne M, Ceresuela J, Rouvet I, Padet S, Acquaviva C, et al. Complete loss of expression of the ANT1 gene causing cardiomyopathy and myopathy. J Med Genet 2012;49: 146–50.
122. Palmieri L, Alberio S, Pisano I, Lodi T, Meznaric-Petrusa M, Zidar J, et al. Complete loss-of-function of the heart/muscle-specific adenine nucleotide translocator is associated with mitochondrial myopathy and cardiomyopathy. Hum Mol Genet 2005;14:3079–88.
123. Körver-Keularts IMLW, de Visser M, Bakker HD, Wanders RJA, Vansenne F, Scholte HR, et al. Two novel mutations in the SLC25A4 gene in a patient with mitochondrial myopathy. JIMD Rep 2015;22:39–45. Springer.
124. Kaukonen J, Juselius JK, Tiranti V, Kyttala A, Zeviani M, Comi GP, et al. Role of adenine nucleotide translocator 1 in mtDNA maintenance. Science 2000;289:782–5.

125. Napoli L, Bordoni A, Zeviani M, Hadjigeorgiou GM, Sciacco M, Tiranti V, et al. A novel missense adenine nucleotide translocator-1 gene mutation in a greek adPEO family. Neurology 2001;57:2295–8.
126. Komaki H, Fukazawa T, Houzen H, Yoshida K, Nonaka I, Goto Y-I. A novel D104G mutation in the adenine nucleotide translocator 1 gene in autosomal dominant progressive external ophthalmoplegia patients with mitochondrial DNA with multiple deletions. Ann Neurol 2002;51:645–8.
127. Punzi G, Porcelli V, Ruggiu M, Hossain MF, Menga A, Scarcia P, et al. SLC25A10 biallelic mutations in intractable epileptic encephalopathy with complex I deficiency. Hum Mol Genet 2018; 27:499–504.
128. Buffet A, Morin A, Castro-Vega L-J, Habarou F, Lussey-Lepoutre C, Letouzé E, et al. Germline mutations in the mitochondrial 2-oxoglutarate/malate carrier SLC25A11 gene confer a predisposition to metastatic paragangliomas. Canc Res 2018; 78:1914–22.
129. Falk MJ, Li D, Gai X, McCormick E, Place E, Lasorsa FM, et al. AGC1 deficiency causes infantile epilepsy, abnormal myelination, and reduced N-acetylaspartate. JIMD Rep 2014;14:77–85. Springer.
130. Wibom R, Lasorsa FM, Töhönen V, Barbaro M, Sterky FH, Kucinski T, et al. AGC1 deficiency associated with global cerebral hypomyelination. N Engl J Med 2009;361:489–95.
131. Kobayashi K, Sinasac DS, Iijima M, Boright AP, Begum L, Lee JR, et al. The gene mutated in adult-onset type II citrullinaemia encodes a putative mitochondrial carrier protein. Nat Genet 1999;22:159–63.
132. Tomomasa T, Kobayashi K, Kaneko H, Shimura H, Fukusato T, Tabata M, et al. Possible clinical and histologic manifestations of adult-onset type II citrullinemia in early infancy. J Pediatr 2001;138:741–3.
133. Yasuda T, Yamaguchi N, Kobayashi K, Nishi I, Horinouchi H, Jalil MA, et al. Identification of two novel mutations in the SLC25A13 gene and detection of seven mutations in 102 patients with adult-onset type II citrullinemia. Hum Genet 2000;107:537–45.
134. Fiermonte G, Soon D, Chaudhuri A, Paradies E, Lee PJ, Krywawych S, et al. An adult with type 2 citrullinemia presenting in Europe. N Engl J Med 2008;358:1408–9.
135. Ohura T, Kobayashi K, Tazawa Y, Nishi I, Abukawa D, Sakamoto O, et al. Neonatal presentation of adult-onset type II citrullinemia. Hum Genet 2001;108:87–90.
136. Tamamori A, Okano Y, Ozaki H, Fujimoto A, Kajiwara M, Fukuda K, et al. Neonatal intrahepatic cholestasis caused by citrin deficiency: severe hepatic dysfunction in an infant requiring liver transplantation. Eur J Pediatr 2002;161:609–13.
137. Tazawa Y, Kobayashi K, Ohura T, Abukawa D, Nishinomiya F, Hosoda Y, et al. Infantile cholestatic jaundice associated with adult-onset type II citrullinemia. J Pediatr 2001;138:735–40.
138. Camacho JA, Obie C, Biery B, Goodman BK, Hu CA, Almashanu S, et al. Hyperornithinaemia-hyperammonaemia-homocitrullinuria syndrome is caused by mutations in a gene encoding a mitochondrial ornithine transporter. Nat Genet 1999;22:151–8.
139. Camacho JA, Mardach R, Rioseco-Camacho N, Ruiz-Pesini E, Derbeneva O, Andrade D, et al. Clinical and functional characterization of a human ORNT1 mutation (T32R) in the hyperornithinemia-hyperammonemia-homocitrullinuria (HHH) syndrome. Pediatr Res 2006;60:423–9.
140. Miyamoto T, Kanazawa N, Kato S, Kawakami M, Inoue Y, Kuhara T, et al. Diagnosis of Japanese patients with HHH syndrome by molecular genetic analysis: a common mutation, R179X. J Hum Genet 2001;46:260–2.
141. Nakajima M, Ishii S, Mito T, Takeshita K, Takashima S, Takakura H, et al. Clinical, biochemical and ultrastructural study on the pathogenesis of hyperornithinemia-hyperammonemia-homocitrullinuria syndrome. Brain Dev 1988;10:181–5.
142. Salvi S, Santorelli FM, Bertini E, Boldrini R, Meli C, Donati A, et al. Clinical and molecular findings in hyperornithinemia-hyperammonemia-homocitrullinuria syndrome. Neurology 2001;57:911–4.
143. Rosenberg MJ, Agarwala R, Bouffard G, Davis J, Fiermonte G, Hilliard MS, et al. Mutant deoxynucleotide carrier is associated with congenital microcephaly. Nat Genet 2002;32:175–9.
144. Spiegel R, Shaag A, Edvardson S, Mandel H, Stepensky P, Shalev SA, et al. *SLC25A19* mutation as a cause of neuropathy and bilateral striatal necrosis. Ann Neurol 2009;66:419–24.
145. Huizing M, Wendel U, Ruitenbeek W, Iacobazzi V, Ijlst L, Veenhuizen P, et al. Carnitine-acylcarnitine carrier deficiency: identification of the molecular defect in a patient. J Inherit Metab Dis 1998;21:262–7.
146. Huizing M, Iacobazzi V, Ijlst L, Savelkoul P, Ruitenbeek W, Van Den Heuvel L, et al. Cloning of the human carnitine-acylcarnitine carrier cDNA and identification of the molecular defect in a patient. Am J Hum Genet 1997;61:1239–45.
147. Costa C, Costa JM, Nuoffer JM, Slama A, Boutron A, Saudubray JM, et al. Identification of the molecular defect in a severe case of carnitine-acylcarnitine carrier deficiency. J Inherit Metab Dis 1999;22:267–70.
148. Ogawa A, Yamamoto S, Kanazawa M, Takayanagi M, Hasegawa S, Kohno Y. Identification of two novel mutations of the carnitine/acylcarnitine translocase (CACT) gene in a patient with CACT deficiency. J Hum Genet 2000;45:52–5.
149. Stanley CA, Hale DE, Berry GT, Deleeuw S, Boxer J, Bonnefont J-P. A deficiency of carnitine–acylcarnitine translocase in the inner mitochondrial membrane. N Engl J Med 1992;327:19–23.
150. Fukushima T, Kaneoka H, Yasuno T, Sasaguri Y, Tokuyasu T, Tokoro K, et al. Three novel mutations in the carnitine-acylcarnitine translocase (CACT) gene in patients with CACT deficiency and in healthy individuals. J Hum Genet 2013;58:788–93.
151. Al Aqeel AI, Rashid MS, Pn Ruiter J, Ijlst L, Ja Wanders R. A novel molecular defect of the carnitine acylcarnitine translocase gene in a Saudi patient. Clin Genet 2003;64:163–5.
152. Iacobazzi V, Pasquali M, Singh R, Matern D, Rinaldo P, di San Filippo CA, et al. Response to therapy in carnitine/acylcarnitine translocase (CACT) deficiency due to a novel missense mutation. Am J Med Genet 2004;126A:150–5.
153. Boczonadi V, King MS, Smith AC, Olahova M, Bansagi B, Roos A, et al. Mitochondrial oxodicarboxylate carrier deficiency is associated with mitochondrial DNA depletion and spinal muscular atrophy-like disease. Genet Med 2018;20:1224–35.
154. Molinari F, Kaminska A, Fiermonte G, Boddaert N, Raas-Rothschild A, Plouin P, et al. Mutations in the mitochondrial glutamate carrier *SLC25A22* in neonatal epileptic encephalopathy with suppression bursts. Clin Genet 2009;76:188–94.
155. Molinari F, Raas-Rothschild A, Rio M, Fiermonte G, Encha-Razavi F, Palmieri L, et al. Impaired mitochondrial glutamate transport

in autosomal recessive neonatal myoclonic epilepsy. Am J Hum Genet 2005;76:334–9.
156. Poduri A, Heinzen EL, Chitsazzadeh V, Lasorsa FM, Elhosary PC, LaCoursiere CM, et al. *SLC25A22* is a novel gene for migrating partial seizures in infancy. Ann Neurol 2013;74:873–82.
157. Adolphs N, Klein M, Haberl EJ, Graul-Neumann L, Menneking H, Hoffmeister B. Necrotizing soft tissue infection of the scalp after fronto-facial advancement by internal distraction in a 7-year old girl with Gorlin–Chaudhry–Moss syndrome – a case report. J Cranio-Maxillofacial Surg 2011;39:554–61.
158. Ehmke N, Graul-Neumann L, Smorag L, Koenig R, Segebrecht L, Magoulas P, et al. De novo mutations in SLC25A24 cause a craniosynostosis syndrome with hypertrichosis, progeroid appearance, and mitochondrial dysfunction. Am J Hum Genet 2017;101:833–43.
159. Faivre L, Van Kien PK, Madinier-Chappat N, Nivelon-Chevallier A, Beer F, LeMerrer M. Can Hutchinson-Gilford progeria syndrome be a neonatal condition? Am J Med Genet 1999;87:450–2.
160. Castori M, Silvestri E, Pedace L, Marseglia G, Tempera A, Antigoni I, et al. Fontaine–Farriaux syndrome: a recognizable craniosynostosis syndrome with nail, skeletal, abdominal, and central nervous system anomalies. Am J Med Genet Part A 2009; 149A:2193–9.
161. Writzl K, Maver A, Kovačič L, Martinez-Valero P, Contreras L, Satrustegui J, et al. De novo mutations in SLC25A24 cause a disorder characterized by early aging, bone dysplasia, characteristic face, and early demise. Am J Hum Genet 2017;101:844–55.
162. Rodríguez JI, Pérez-Alonso P, Funes R, Pérez-Rodríguez J. Lethal neonatal Hutchinson-Gilford progeria syndrome. Am J Med Genet 1999;82:242–8.
163. Kishita Y, Pajak A, Bolar NA, Marobbio CMT, Maffezzini C, Miniero DV, et al. Intra-mitochondrial methylation deficiency due to mutations in SLC25A26. Am J Hum Genet 2015;97:761–8.
164. Schiff M, Veauville-Merllié A, Su CH, Tzagoloff A, Rak M, Ogier de Baulny H, et al. SLC25A32 mutations and riboflavin-responsive exercise intolerance. N Engl J Med 2016;374:795–7.
165. Guernsey DL, Jiang H, Campagna DR, Evans SC, Ferguson M, Kellogg MD, et al. Mutations in mitochondrial carrier family gene SLC25A38 cause nonsyndromic autosomal recessive congenital sideroblastic anemia. Nat Genet 2009;41:651–3.
166. Almannai M, Alasmari A, Alqasmi A, Faqeih E, Al Mutairi F, Alotaibi M, et al. Expanding the phenotype of *SLC25A42*-associated mitochondrial encephalomyopathy. Clin Genet 2018; 93:1097–102.
167. Iuso A, Alhaddad B, Weigel C, Kotzaeridou U, Mastantuono E, Schwarzmayr T, et al. A homozygous splice site mutation in SLC25A42, encoding the mitochondrial transporter of coenzyme a, causes metabolic crises and epileptic encephalopathy. JIMD Rep 2019;44:1–7. Springer.
168. Shamseldin HE, Smith LL, Kentab A, Alkhalidi H, Summers B, Alsedairy H, et al. Mutation of the mitochondrial carrier SLC25A42 causes a novel form of mitochondrial myopathy in humans. Hum Genet 2016;135:21–30.
169. Abrams AJ, Hufnagel RB, Rebelo A, Zanna C, Patel N, Gonzalez MA, et al. Mutations in SLC25A46, encoding a UGO1-like protein, cause an optic atrophy spectrum disorder. Nat Genet 2015;47: 926–32.
170. Wan J, Steffen J, Yourshaw M, Mamsa H, Andersen E, Rudnik-Schöneborn S, et al. Loss of function of SLC25A46 causes lethal congenital pontocerebellar hypoplasia. Brain 2016;139:2877–90.
171. Charlesworth G, Balint B, Mencacci NE, Carr L, Wood NW, Bhatia KP. *SLC25A46* mutations underlie progressive myoclonic ataxia with optic atrophy and neuropathy. Mov Disord 2016;31: 1249–51.
172. Janer A, Prudent J, Paupe V, Fahiminiya S, Majewski J, Sgarioto N, et al. SLC25A46 is required for mitochondrial lipid homeostasis and cristae maintenance and is responsible for Leigh syndrome. EMBO Mol Med 2016;8:1019–38.
173. Esterbauer H, Schneitler C, Oberkofler H, Ebenbichler C, Paulweber B, Sandhofer F, et al. A common polymorphism in the promoter of UCP2 is associated with decreased risk of obesity in middle-aged humans. Nat Genet 2001;28:178–83.
174. Bulotta A, Ludovico O, Coco A, Di Paola R, Quattrone A, Carella M, et al. The common −866G/A polymorphism in the promoter region of the UCP-2 gene is associated with reduced risk of type 2 diabetes in Caucasians from Italy. J Clin Endocrinol Metab 2005;90:1176–80.
175. Argyropoulos G, Brown AM, Willi SM, Zhu J, He Y, Reitman M, et al. Effects of mutations in the human uncoupling protein 3 gene on the respiratory quotient and fat oxidation in severe obesity and type 2 diabetes. J Clin Invest 1998;102:1345–51.
176. Brown AM, Willi SM, Argyropoulos G, Garvey WT. A novel missense mutation, R70W, in the human uncoupling protein 3 gene in a family with type 2 diabetes. Hum Mutat 1999;13:506.
177. Pettersen EF, Goddard TD, Huang CC, Couch GS, Greenblatt DM, Meng EC, et al. UCSF Chimera – a visualization system for exploratory research and analysis. J Comput Chem 2004;25: 1605–12.